Clim Dyn (2018) 51:57–71
DOI 10.1007/s00382-017-3906-4

Tibetan Plateau capacitor effect during the summer preceding ENSO: from the Yellow River climate perspective

Rui Jin[1] · Zhiwei Wu[2] · Peng Zhang[1]

Received: 25 April 2017 / Accepted: 7 September 2017 / Published online: 13 September 2017

Abstract It is well recognized that El Niño-Southern Oscillation (ENSO) may exert a direct impact on the East Asian summer monsoon rainfall through modulating the Philippine Sea anticyclone variability. Such ENSO associated influence is evident in the monsoon region, i.e., Southeast China, the Yangtze River, Korean Peninsula and Japan. It remains unclear whether and how this ENSO related effect can reach the Yellow River region, a monsoon/arid transition region. In this study, results show that the year-to-year variations of the Yellow River summer rainfall can be indirectly influenced by ENSO, during its developing phase. The western Tibetan Plateau snow cover (WTPSC) may act as a "capacitor", helping ENSO signal to reach the Yellow River region. During the El Niño developing spring, the associated diabatic heating in Pacific region can excite an anomalous cyclone over the plateau and anomalous upward flows over the western plateau. Such circulation configuration favors an excessive WTPSC anomaly in spring. The more WTPSC may increase the surface albedo, decrease the absorbed net shortwave radiation and in turn intensify the WTPSC. Through such snow-albedo feedback process, the excessive WTPSC anomaly may strengthen and persist through summer, which may induce two noticeable wave trains in the upper and lower troposphere propagating northeastward to the Yellow River region. Associated with the wave trains, a low pressure anomaly prevails over northeast China. To the southwest side of the anomalous low pressure, the abnormal northerly wind may bring large volumes of dry cold air with little moisture to the Yellow River region, leading to the anomalous drought there. During the La Niña developing summer, the situation tends to be opposite. As such, the ENSO associated influence is tied to the interannual variations of the following summer Yellow River precipitation, with the development of ENSO from spring.

✉ Zhiwei Wu
zhiweiwu@fudan.edu.cn

[1] College of Atmospheric Science and Key Laboratory of Meteorological Disaster of Ministry of Education, Nanjing University of Information Science and Technology, Nanjing 210044, Jiangsu, China

[2] Institute of Atmospheric Sciences (IAS), Fudan University, Shanghai 200433, China

1 Introduction

As the dominant interannual mode of tropical oceans, it is demonstrated that El Niño-Southern Oscillation (ENSO) may seriously impact the Asian summer monsoon (ASM) precipitation (Shukla and Paolino 1983; Huang and Wu 1989; Webster and Yang 1992; Wang et al. 2000, 2003 ; Ropelewski and Halpert 1987; Chang et al. 2000; Xie et al. 2009; Feng et al. 2016; Li 2009). Hence, ENSO has been regarded as a crucial predictability source for the interannual variations of the summer rainfall in the Asian monsoon regions, including Southeast China, the Yangtze River, Korean Peninsula and Japan (Kawamura 1998; Wang et al. 2000, 2003; Ju and Slingo 1995). Nevertheless, for the monsoon/arid transition area in the Yellow River, such ENSO associated effect may not be quite clear. In summer (June−September), the Yellow River rainfall takes up more than 70% of the annual total (Huang et al. 2011), making it a crucial stage for the agricultural industry there. Precise forecast of the Yellow River summer rainfall is then obviously of great societal and scientific value. Thus, a critical open question is that to what extent this interannual variation of the Yellow River summer precipitation can be attributed to ENSO and what is the physical mechanism.

Some studies suggested a potential link between ENSO and the Yellow River rainfall variations (Huang and Wu 1989; Zhang et al. 1999). For instance, Nitta (1987) investigated the characteristic of the Pacific Japan (PJ) pattern, featured by the meridional dipole mode of the teleconnection pattern in the western Pacific region. This structure may connect ENSO to the large variations in East Asia summer rainfall over higher latitude regions. However, according to Huang (2004), the impact of PJ pattern may not reach the Yellow River region. Feng and Hu (2004) revealed another conceivable mechanism, which pointed out the possible ENSO impact on the Yellow River summer rainfall via modulating the Indian summer monsoon (ISM) variability. It has been long known that ENSO event may have obvious impacts on ISM rainfall (Webster and Yang 1992; Kawamura 1998; Yang 1996; Ju and Slingo 1995). Besides, possible connections between ISM and the Yellow River summer rainfall were also proposed (Guo and Wang 1988; Kripalani and Singh 1993; Zhang 1999; Yatagai and Yasunari 1995; Kripalani and Kulkarni 1997), which may be attributed to the modulation of Eurasia teleconnection patterns (EU) (Wang et al. 2001; Wu and Wang 2002). Moreover, in the recent study, Ding and Wang (2005) revealed a significant summertime circum-global teleconnection (CGT) pattern over the mid-latitude regions in Northern Hemisphere. The CGT is primarily located in the region where the westerly jet stream prevails. When the ENSO-ISM interaction is active, the previous ENSO associated influence may extend to the Yellow River region in summer via the effect of CGT. However, located in the mid-latitude regions, the interannual variation of the Yellow River summer rainfall is quite complicated (Feng et al. 2011; Yatagai and Yasunari 1995; Yang and Lau 2004), owing to some other factors, e.g., the Tibetan Plateau (TP) thermal effect, the westerly jet stream and North Atlantic Oscillation (Qian et al. 2003; Zhang et al. 2004; Liang and Wang 1998; Zheng et al. 2016; Wu et al. 2009; Li et al. 2013). These factors may more or less have some connections with ENSO. Thus, credible conclusions of how ENSO may affect the Yellow River summer rainfall have not been reached so far.

With its mean elevation over 4000 m, TP is one of the primary forcing factors in mid-latitudes and may shape the climate change in the Northern Hemisphere or even the global (Ren et al. 2010; Murakami and Ding 1982; Duan and Wu 2005; Wu et al. 1997, 2007; Wang et al. 2008; Liu et al. 2007; Zhang and Tao 2001; Wu and Liu 2003). Snow cover is a crucial factor measuring the TP land surface thermal condition. Owing to the towering mountain, the western Tibetan Plateau snow cover (WTPSC) may persist through summer (Pu et al. 2007) and impact the climate change over the Yellow River and its surrounding areas (Wu et al. 2012b, 2015; Liu et al. 2014), which is quite different from the Eurasian snow cover (Wu and Zhang 1998; Zhang et al. 2004; Lin and Wu 2011; Wu et al. 2012a). For example, Wu et al. (2012b, 2015) considered that the increase of summer heat wave activities in northern China or even the Eurasian continent can be highly attributed to the reduced WTPSC.

Except for this close linkage between TP and the Yellow River summer climate, the interannual variations of the TP thermal effect is found significantly affected by ENSO events. Miyakoda et al. (2003) suggested that there was a circulation anomaly over TP in spring associated with ENSO, which may modulate the surface air temperature, soil moisture, snow depth and snow cover there (Shaman and Tziperman 2005; Dong and Valdes 1998; Liu et al. 2015). On account of these observations, Shaman and Tziperman (2005) referred an ENSO associated atmospheric stationary wave train in the troposphere across the Eurasia, which was utilized to illuminate the influence of ENSO on the circulation anomaly over TP. Besides, Liu et al. (2015) focused on the crucial role of this ENSO related summertime north Indian Ocean thermal effect in modulating the circulation over TP. These studies all present the possible linkage between ENSO and the TP snow cover.

Having known the important climate impact of the WTPSC on the Yellow River summer climate as well as its connection to preceding ENSO, it is reasonable to speculate whether the interannual variations of the Yellow River summer rainfall may be influenced by ENSO through the "capacitor" effect of the WTPSC. Therefore, the following two issues will be concentrated on: (1) Can ENSO signal affect the Yellow River summer precipitation? (2) What contribution would the WTPSC make in this process? The study's frame is organized as follows. Descriptions of the applied datasets, model and methodology are described in Sect. 2. Section 3 reveals the possible impact of ENSO on the WTPSC and their combined effect on the Yellow River summer precipitation. Section 4 proposes the possible mechanism as well as the model result. Finally, the major findings, as well as some discussions, will be presented in Sect. 5.

2 Datasets, model, and methodology

Datasets applied in this paper are shown as follows: the monthly dataset of the Tibetan Plateau snow cover provided by the Global Snow Lab (Rutgers University) (http://climate.rutgers.edu/snowcover) during 1970−2014 (Robinson et al. 1993; Robinson and Frei 2000); the monthly sea surface temperature (SST) data supplied by the National Oceanic and Atmospheric Administration (NOAA) Extended Reconstructed SST Version3 (ERSST V3) (Smith et al. 2008); the precipitation data derived from the NOAA's Precipitation Reconstruction (PREC) (Chen et al. 2002); the reanalysis data during 1970−2014 by the

Table 1 Experiment designs

Experiment	Prescribed SST
EXP-CTRL	Spring (MAM) climatological SSTs
EXP-TPA (EN)	Climatological SSTs + composite SSTA of El Niño in only Pacific (MAM)
EXP-TPA (LN)	Climatological SSTs + composite SSTA of La Niña in only Pacific (MAM)

National Centers for Environmental Prediction-National Center for Atmospheric Research (NCEP-NCAR) (Kalnay et al. 1996). Also provided is the monthly albedo data by the ERA Twentieth Century Reanalysis Project for 1970–2010 (Poli et al. 2016).

An Atmospheric General Circulation Model (AGCM), the 5th generation European Centre-Max Plank Institute model (ECHAM), v5.4 (Roeckner et al. 2003) is employed to illuminate the possible mechanism. It is a general circulation program that has been widely used in former studies. The resolution we used in present study is triangular 42, with 19 vertical levels (T42L19). Based on

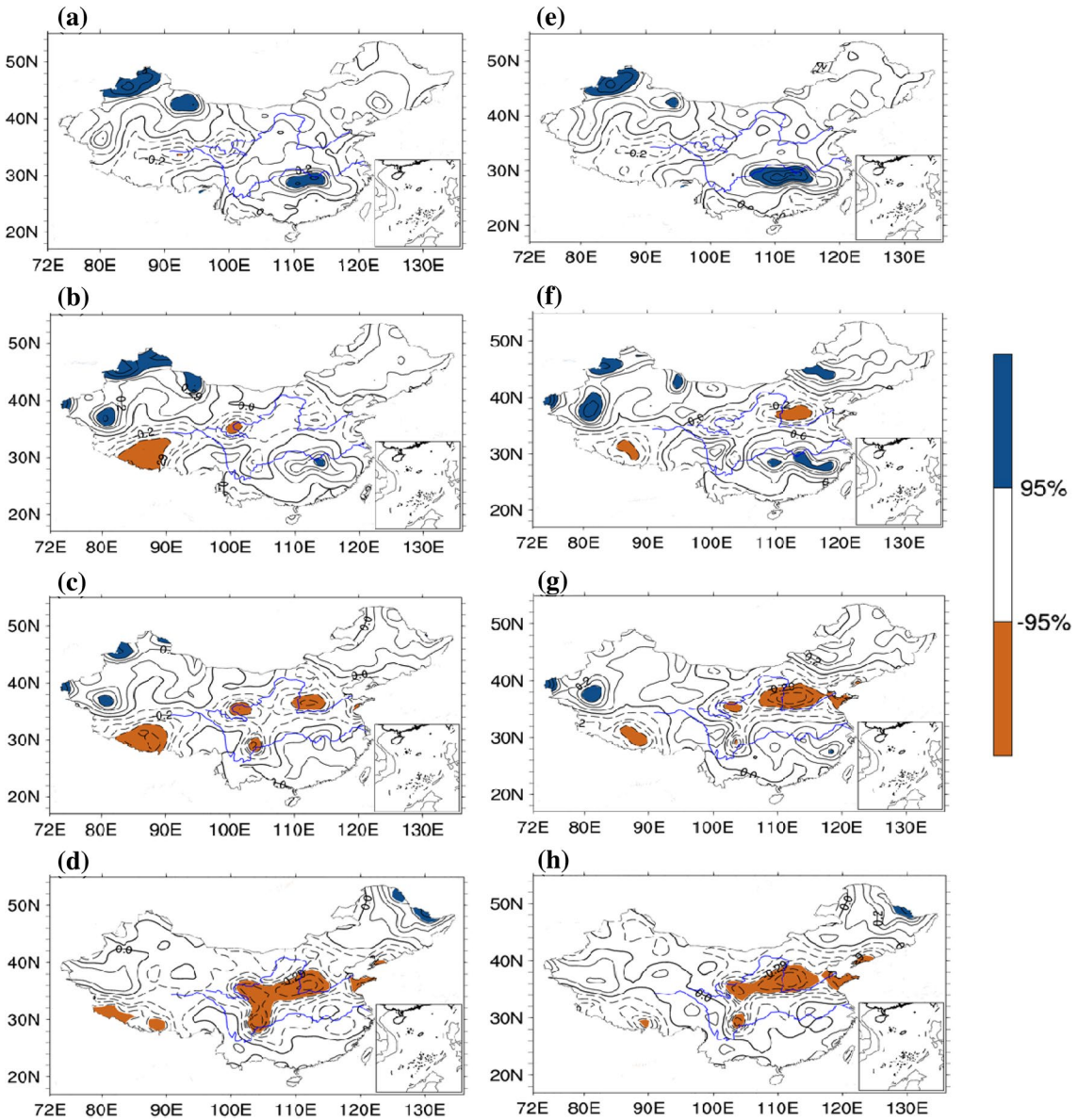

Fig. 1 Correlation maps between the summer [June–September (JJAS)] precipitation and the preceding Niño 3.4 index (**a**–**d**)/Niño 3 index (**e**–**h**). **a, e** DJF, **b, f** MAM, **c, g** AMJ, and **d, h** JJAS. The positive (negative) values significant at the 95% confident level are shaded with blue (yellow)

this model, three experiments are performed: firstly, we design a control experiment with AMIP II historical SST prescribed for ten randomly chosen sample years. Each sample is integrated for 3 years, and the last year result is analyzed. Then, the SST anomaly sensitivity experiments are performed, adding the observational SST anomalies to the spring time (MAM) historical SSTs. The simulations are integrated from 31 January to 31 May for each year with the initial fields taken from the control experiment. Taking the year of 1959 as an example, the control experiment is integrated from 1 January 1957 to 31 May 1959, and the results from 1 March to 31 May in 1959 are used as samples. The sensitivity experiment is integrated from 1 February to 31 May and the results of the last 3 months are used. The detailed designs are shown in Table 1. The Pacific region where SSTA is used in the simulation is bounded by 120°−270°E and −40°S−40°N.

To avoid the interference of the linear trends, the snow cover datasets and ENSO index are detrended. Statistical methods, such as correlation, partial correlation, regression, and composite are also employed. The Niño3.4 index is the mean SST anomaly (SSTA) of the area bounded by 5°S–5°N and 170°–120°W, while the Niño 3 index is bounded by 5°S–5°N and 150°–90°W. Seasonal mean are computed for winter (DJF) from December to February, spring (MAM) from March to May and summer (JJAS) from June to September.

3 ENSO, TP snow cover, and the Yellow River summer rainfall

Figure 1a–d give out the correlation maps of summer (JJAS) rainfall over China with reference to the previous winter (DJF), spring (MAM, AMJ) and summer (JJAS) Niño 3.4

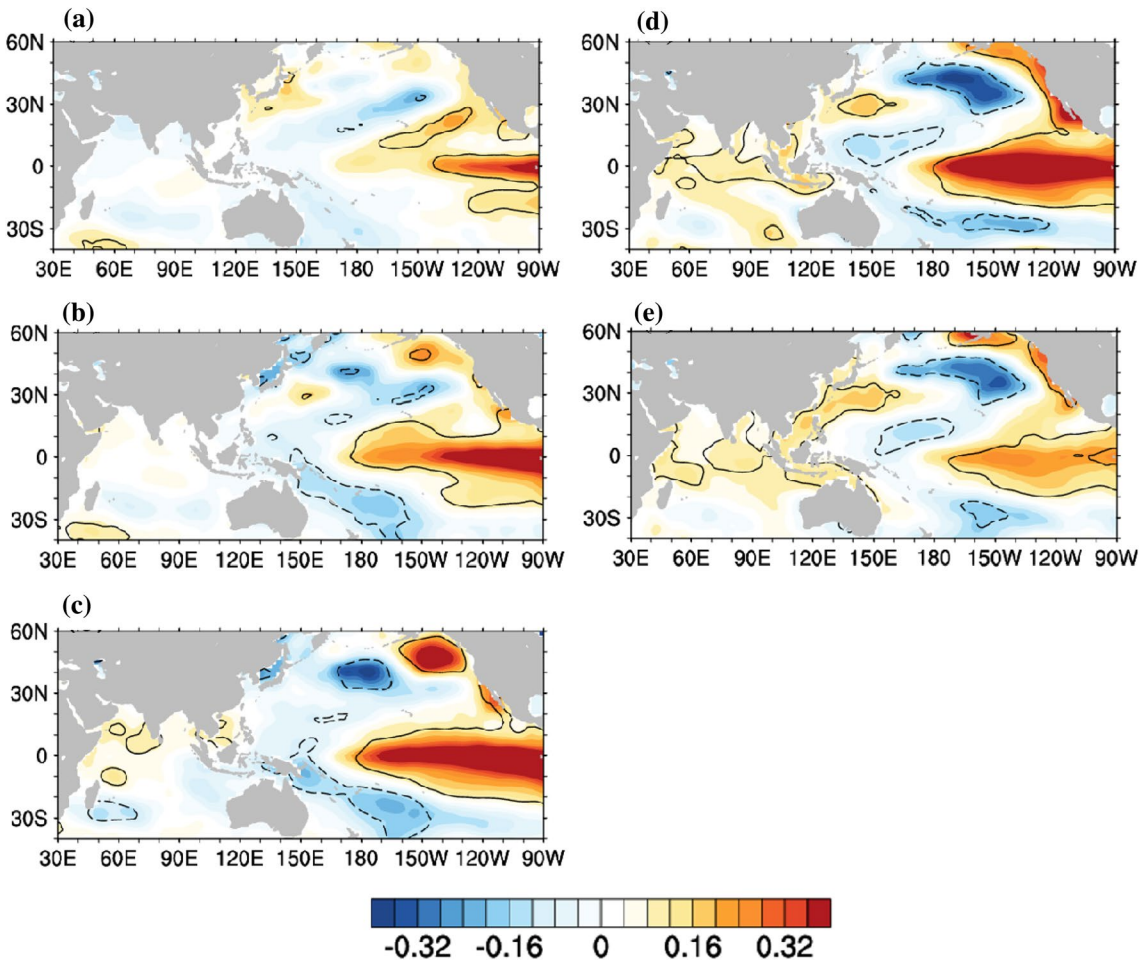

Fig. 2 **a** MAM(0), **b** JJA(0), **c** SON(0), **d** D(0)JF(+1) and **e** MAM(+1) SST (k) (shading) regressed against the Yellow River summer rainfall index (YRRI) [JJAS(0)]. "0" represents the simultaneous year while "+1" is the next year. The black solid (dashed) curves represent positive (negative) values significant at the 95% confident level

index. The same is true for Niño 3 index (Fig. 1e–h). Corresponding to the numerous studies, large regions of positive correlations occupy the Yangtze River in Fig. 1a, e, which diminish with the evolution from spring to summer. This phenomenon means that the previous winter ENSO may impact on the following summer Yangtze River precipitation through modulating the Philippine Sea anticyclone variation during its decaying phase (Wang et al. 2000; Chang et al. 2000). However, the situation changes if we focus on the Yellow River region. Negative correlations occupy the Yellow River region from spring, especially those by using ENSO index in late spring (AMJ) and summer (JJAS) (Fig. 1c, d, g, h). That means the relationship between the Yellow River summer rainfall and ENSO establishes in spring and further strengthens in the following summer, with the development of ENSO. If we define the average summer (JJAS) precipitation in the area bounded by 35°N–39°N and 98°–124°E as the Yellow River summer rainfall index (YRRI), the correlations between the YRRI and Niño 3.4/ Niño 3 index (AMJ) reach −0.4 and −0.49, both exceeding the 99% confident level. Thus, ENSO signal in spring can be used for predicting the following summer Yellow River precipitation.

To further explain the relationship between ENSO and the Yellow River summer rainfall. Seasonal evolutions of the SST patterns associated with the negative YRRI (JJAS) are presented (Fig. 2). "0" represents the simultaneous year while "+1" is the next year here. The changes of SST anomalies indicate the ENSO developing progress. Warm SST anomalies begin to establish in spring, with the strongest anomalies shown in the following autumn and winter. During the next spring, ENSO diminishes. This further supports the result that ENSO may influence the following summer Yellow River rainfall during its developing stage. Since the Yellow River region is located in a monsoon/arid transition area, far from the tropical region. Then, how can ENSO impact on the Yellow River precipitation?

Except for the distinctive impact of ENSO on the Yellow River rainfall, the TP snow cover variability may also highly contribute to the summer climate change in the Yellow River region according to the previous researches (Wu et al. 2012b; Qian et al. 2003; Zhang et al. 2004; Liu et al. 2014). Thus, a hypothesis is raised that whether the TP snow cover may act as a "capacitor" linking ENSO and the Yellow River summer rainfall, during the ENSO developing phase.

To further study the characteristic as well as the climate effect of TP snow cover, Fig. 3a gives out the climatology and standard deviation (STD) of summer (JJAS) TP snow cover for the period of 1970−2014. Over the western and southern TP regions, heavy snow cover lays in summer owing to the great mountain ridges. Coincidentally, these snow cover areas happen to occupy the strong STD centers. Therefore, notable interannual variations in the WTPSC are observed, which may lead to the climate change in northern China or even the Eurasia continent, according to the results of Wu et al. (2012a, 2015).

In accordance with this distinct feature of the summertime TP snow cover, we define a WTPSC index (WTPSI), which is the average snow cover in the area bounded by 33°N–43°N and 70°E–78°E. The preceding spring (MAM) and summer (JJAS) Niño 3.4 index, as well as the normalized summer

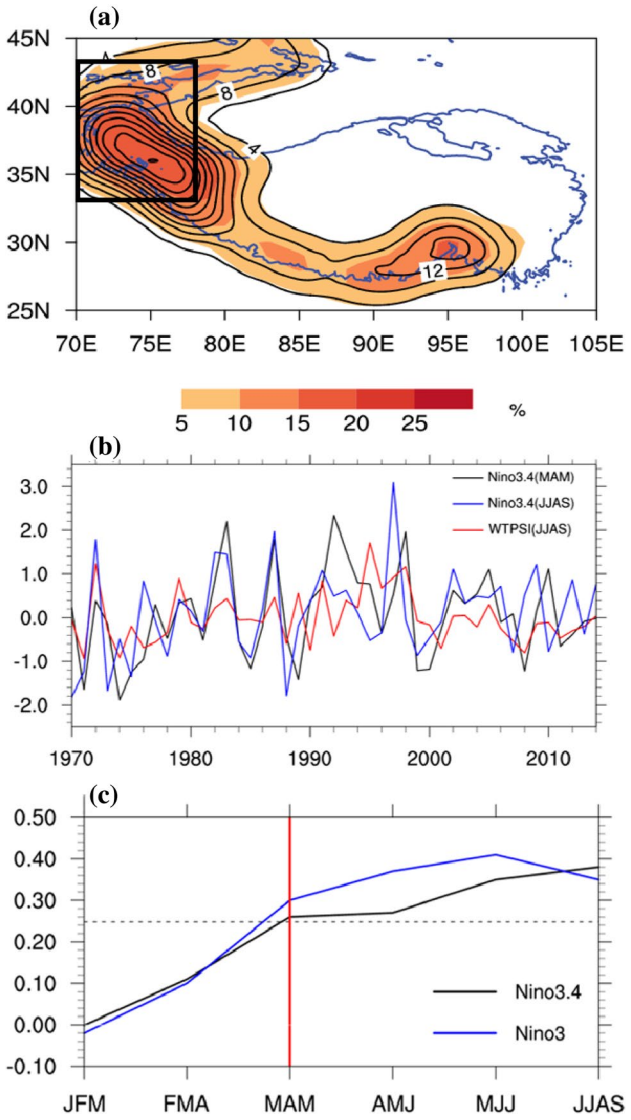

Fig. 3 **a** Long-term mean (%) (contours) and standard deviation (%) (color shadings) of the WTPSC during boreal summer (JJAS) for the period of 1970−2014. The contour interval is 4 (%). **b** The detrended temporal evolution of the normalized WTPSC index (WTPSI) (red curve) defined as the snow cover averaged within the black-boxed area (33°−43°N, 70°−78°E). The black and blue curves indicate the Niño 3.4 index in spring (MAM) and summer (JJAS). **c** The simultaneous correlation coefficients between the WTPSI and Niño 3/ Niño 3.4 index from winter to the following summer. The dashed line represents the 90% significant intervals

WTPSI, with the long term trend removed are shown in Fig. 3b. Pronounced year-to-year variations of these three indices are observed, which may be quite important to the interannual variation of East Asian climate. Moreover, both spring and summer Niño 3.4 index show good relationships with the WTPSI (JJAS), exceeding the 99% confidence level.

To further confirm this ENSO-WTPSC relation, Fig. 3c displays the simultaneous correlation coefficient between the WTPSI and Niño 3/Niño 3.4 index from winter to the following summer. An interesting phenomenon shows that the relationship between ENSO and the WTPSC also establishes in spring (MAM), with the simultaneous correlation coefficients between the WTPSI and Niño 3/Niño 3.4 index exceeding the 90% and 95% confidence level respectively. This connection persists and becomes stronger in the following summertime, which corresponds to the result in Fig. 1. Besides, the SST anomalies associated with the WTPSI are also presented in Fig. 4. Similar to Fig. 2, the changes of SST anomalies with seasons can be regarded as the ENSO developing stage. On account of the regions exceeding the 95% confident level (black curves), the connection between the WTPSC (JJAS) and SST anomalies in equatorial central and eastern Pacific is strongest in the previous spring and the simultaneous summer, further supporting the results in Fig. 3c.

Having known the close linkage between the developing ENSO and the WTPSC, we further identify the possible impact of these two factors on the Yellow River summer precipitation. Similar to Fig. 1, the partial correlation maps between the summer [June–September (JJAS)] precipitation and the preceding spring (MAM, AMJ) and summer (JJAS) Niño 3.4 index with the WTPSI removed have been given out in Fig. 5a–c. The same is true for the correlation maps by using Niño 3 index (Fig. 5d–f). As we can see, compared with Fig. 1, negative correlations in the Yellow River have been diminished a lot by removing the signal of the WTPSC. In other words, without the "capacitor" effect of the WTPSC, the connection between ENSO and the Yellow River summer rainfall may greatly weaken.

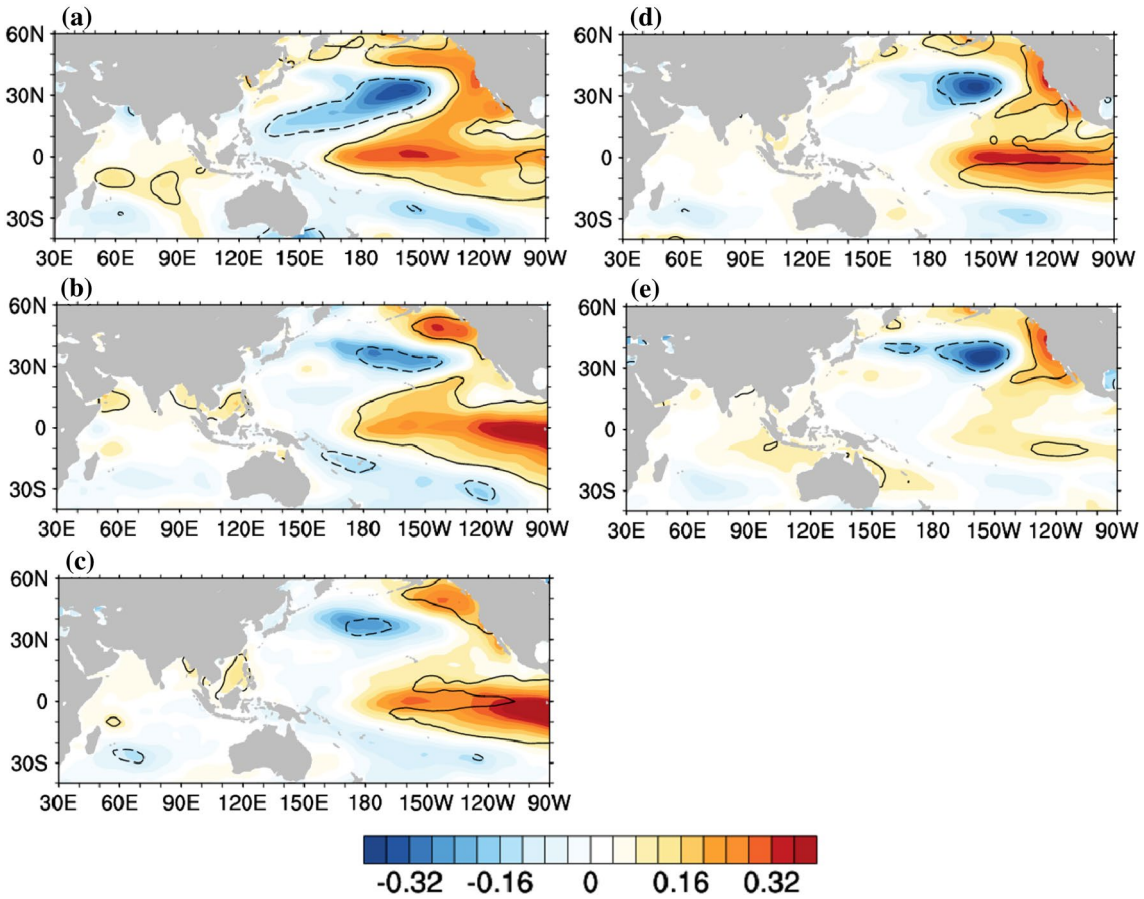

Fig. 4 **a** MAM(0), **b** JJA(0), **c** SON(0), **d** D(0)JF(+1) and **e** MAM(+1) SST (k) (shading) regressed against the WTPSI [JJAS(0)]. "0" represents the simultaneous year while "+1" is the next year. The black solid (dashed) curves represent positive (negative) values significant at the 95% confident level

Besides, the correlation map of summer (JJAS) precipitation in China with reference to the WTPSI (JJAS) is given out (Fig. 6). In East China, negative correlation center prevails in the Yellow River region while the positive one in the Yangtze River. This correlation pattern indicates that the summer precipitation in East China can be largely attributed to this ENSO related WTPSC in summer, particularly those in the Yellow River region.

These results further confirm the important role of this ENSO related summer WTPSC in the Yellow River rainfall and add to the growing body of evidence that a developing ENSO may impact the Yellow River summer rainfall indirectly through the "capacitor" effect of the WTPSC. The detailed physical processes will be addressed in Sect. 4.

4 Physical mechanism

4.1 ENSO impact on the spring WTPSC

The upper wind (200-hPa, UV) for the previous spring (MAM) regressed on the WTPSI is shown in Fig. 7a. For Eurasian continent, an evident cyclonic circulation anomaly prevails mainly over the central and western TP, associated to the positive snow cover abnormity there. When we focus on the Pacific region, the circulation anomalies are characterized by the abnormal north–south dipole anticyclones around the equatorial central and eastern Pacific as well as a cyclonic anomaly over Aleutian, which form the ENSO associated circulation patterns (Matsuno 1966; Gill 1980). Moreover, Fig. 7b presents the regression pattern between the WTPSI and lower wind (850-hPa, UV) in spring. Remarkable westerly anomalies occupy the equatorial central and eastern Pacific, which may favor the El Niño development. Meanwhile, a prominent cyclonic anomaly is

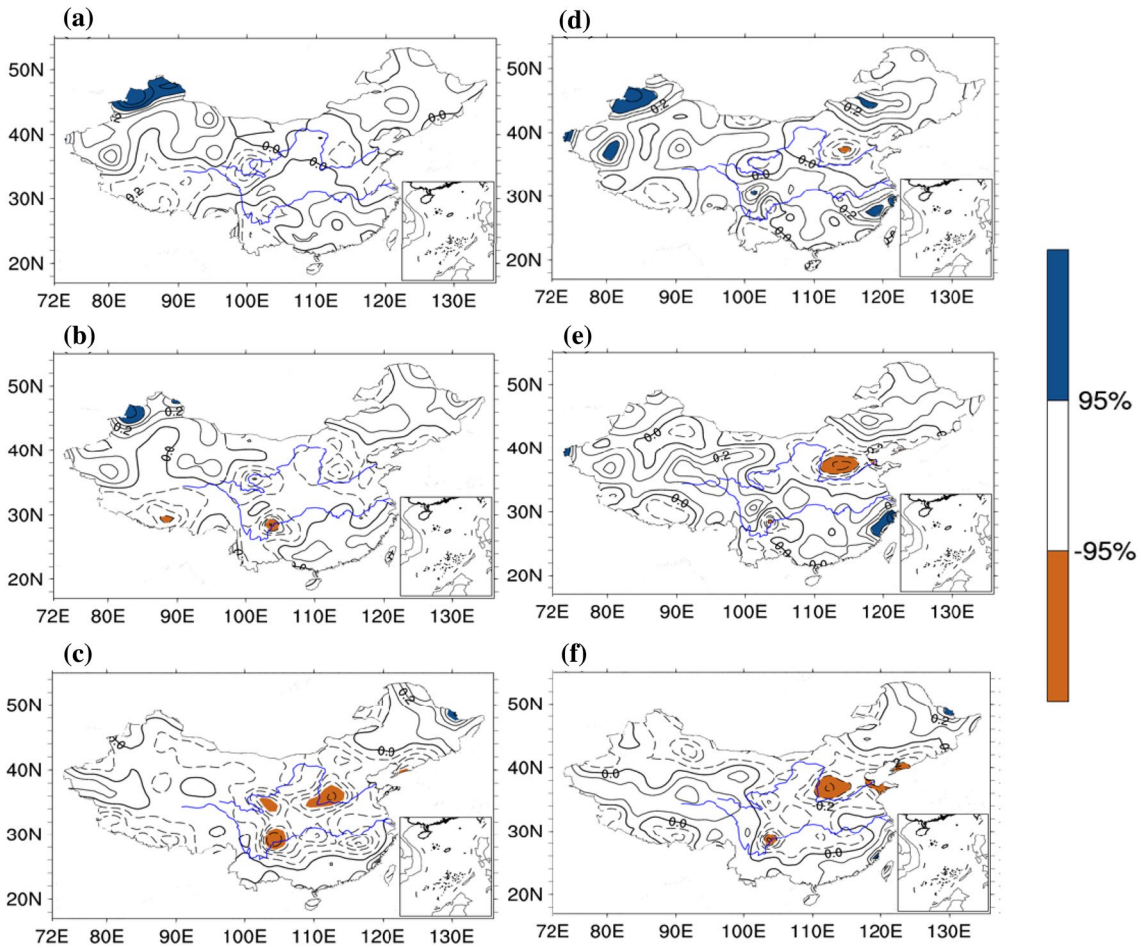

Fig. 5 Partial correlation maps between the summer [June–September (JJAS)] precipitation and Niño 3.4 index (**a**–**c**)/Niño 3 index (**d**–**f**) with the WTPSI removed. **a, d** MAM, **b, e** AMJ, and **c, f** JJAS. The positive (negative) values significant at the 95% confident level are shaded with blue (yellow)

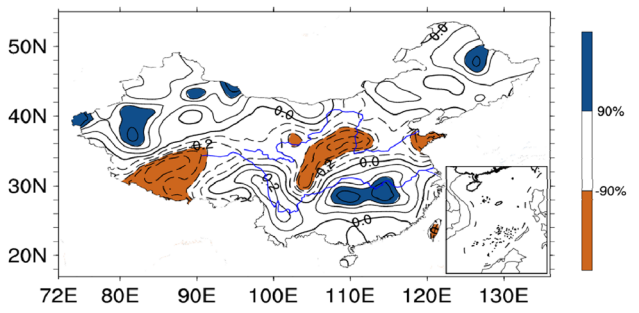

Fig. 6 Correlation map between the WTPSI in summertime (JJSA) and precipitation (JJAS). The positive (negative) values significant at the 90% confident level are shaded with blue (yellow)

located over Aleutian, forming a barotropic structure there. These anomalous circulation patterns in both upper and lower level in Pacific region can be regarded as the direct response to El Niño heating, which further verify that the anomalous WTPSC may be highly associated with the developing ENSO signal. For the WTPSC associated large scale precipitation field, it is characterized by a horseshoe shape (Fig. 7c). Anomalous positive precipitation prevails over the tropical central and eastern Pacific, while negative one located in the western Pacific. Therefore, the upper level (200-hPa) cyclonic anomaly over TP and the WTPSC are highly correlated to those precipitation anomalies in Pacific, especially those in the western north Pacific and Maritime Continent, which may exert great impact on the TP circulation through the Gill-response (Matsuno 1966; Gill 1980). In

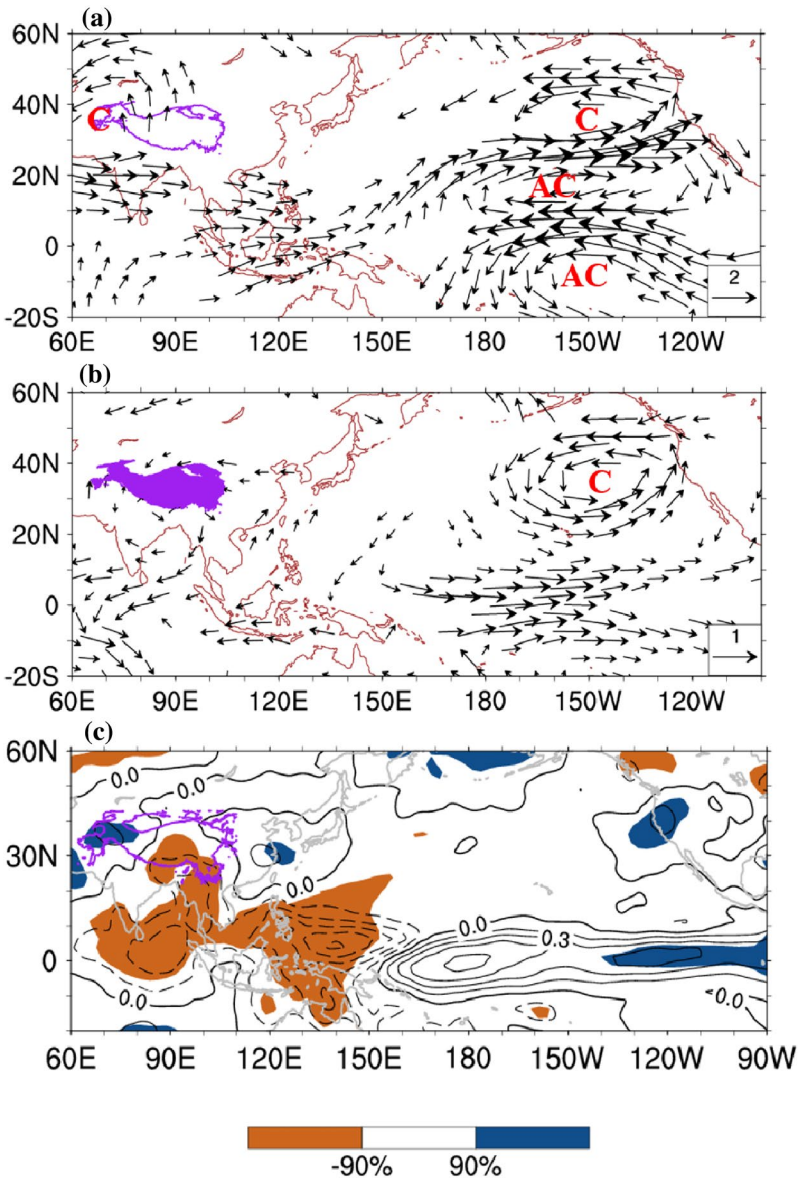

Fig. 7 **a** Upper wind abnormity (200-hPa, UV) (m/s), **b** lower wind abnormity (850 hPa, UV) (m/s), and **c** large scale precipitation abnormity (mm/day) regressed against the WTPSI (JJAS). The purple curves and shadings represent the area above 3000 m. The vectors indicate statistically significant at 95% confidence level. The positive (negative) values significant at the 90% confident level are shaded with blue (yellow) in **c**. The letter AC and C denote anticyclonic and cyclonic circulation centers, respectively

order to further illuminate the importance of the convective anomalies there, the spring (MAM) precipitation anomalies averaged within the tropical western north Pacific and Maritime Continent (−10°−20°N, 90°−150°E) are defined as the western north Pacific precipitation index (WNPI).

To investigate the ENSO associated regional circulation response over TP, Fig. 8a presents the composite difference in the TP snow cover between warm and cold ENSO events in spring, which are defined when Niño 3.4 index is beyond the ±0.7 standardized deviation. Nearly uniform patterns are also shown in regression analysis (figure not shown). In spring, noticeable positive snow cover anomalies in the western TP are noted (Fig. 8a), corresponding to the cyclonic abnormity over TP (Fig. 7a). According to the thermal adaptation (Wu and Liu 2003; Liu et al. 2004; Liu and Wu 2004), the vertical velocity (omega) is proportional to the meridional wind vertical shear in the subtropical regions. Given the high level cyclonic circulation anomalies over the central and western Tibetan Plateau, Fig. 8b presents the composite differences of the meridional wind vertical shear (V100–V400) between the warm and cold ENSO

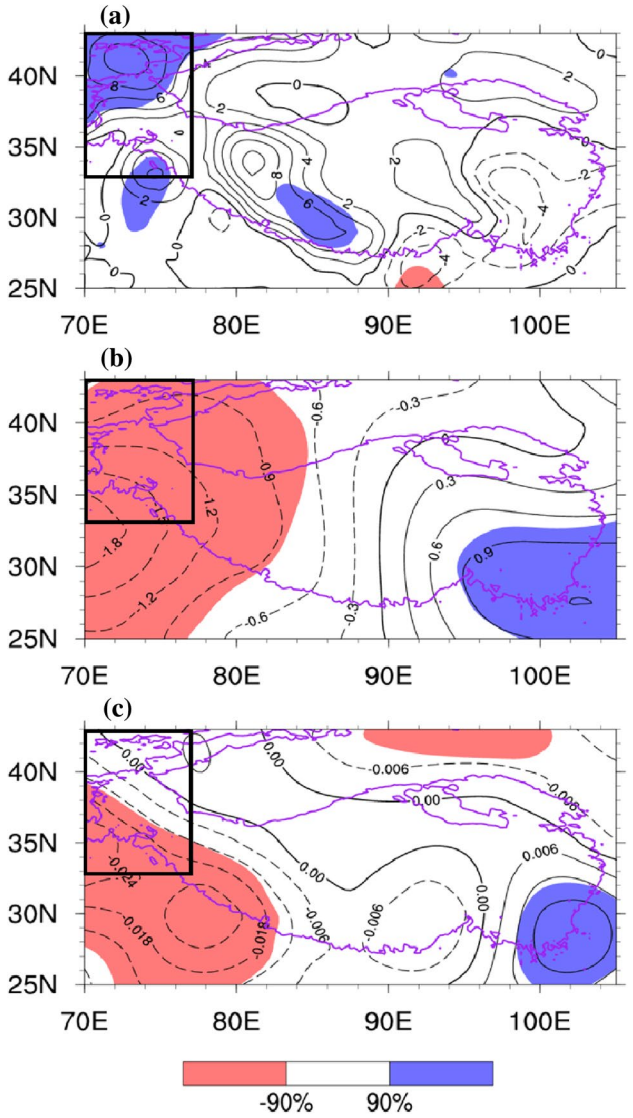

Fig. 8 **a** Composite difference in spring (MAM) snow cover (%) between the warm and cold ENSO events. As in **a**–**c** present composite difference of spring (MAM) meridional wind difference between 100-hPa and 400-hPa (m/s) and the spring (MAM) 400-hPa vertical motion (omega, Pa/s). The purple curve represents the area above 3000 m. The positive (negative) values significant at the 90% confident level are shaded with blue (red)

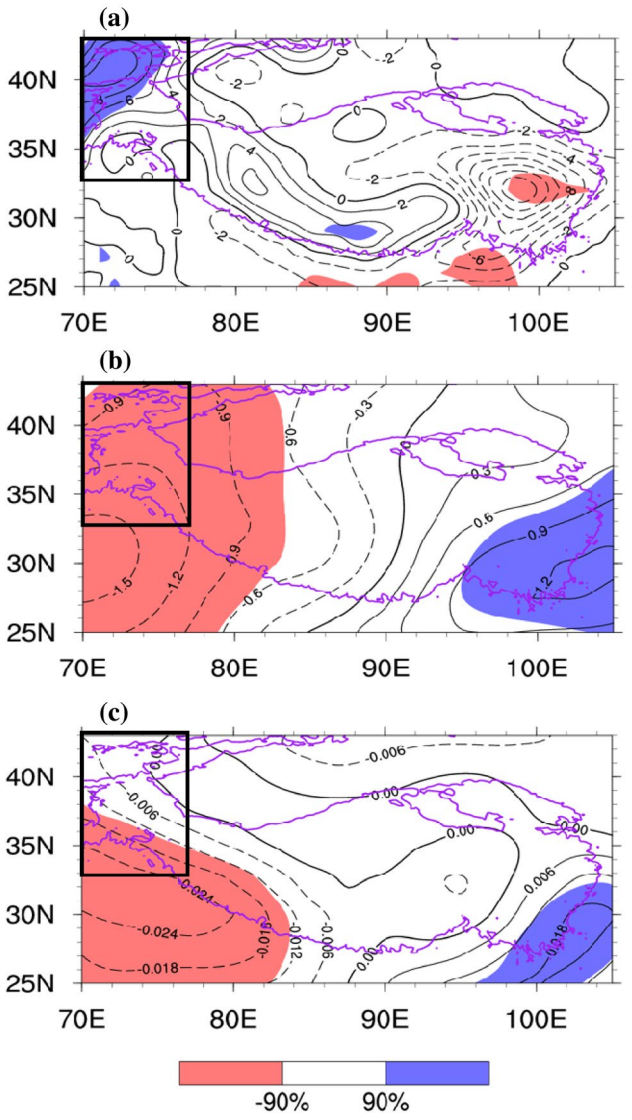

Fig. 9 **a** Composite difference in spring (MAM) snow cover (%) between the low and high WNPI years (defined when WNPI is beyond the ∓0.7standardized deviation). As in **a**–**c** present composite differences of spring (MAM) meridional wind difference between 100-hPa and 400-hPa (m/s) and the spring (MAM) 400-hPa vertical motion (omega, Pa/s). The purple curve represents the area above 3000 m. The positive (negative) values significant at the 90% confident level are shaded with blue (red)

events. Large regions of negative anomalies situate over the western Tibetan Plateau, which may favor the anomalous upward motion there (Fig. 8c). Significant upward anomaly associated to ENSO is displayed in western TP, while weak downward abnormity is positioned in eastern TP, consistent with the WTPSI associated precipitation anomalies over TP (Fig. 7c). Anomalous upward flows in western TP occupy the key area of the WTPSI (Fig. 3a) and favor the convective activities there. This circumstance further suggests that the WTPSC variability may be closely linked with those ENSO associated circulation anomaly in spring, featured by the upper level cyclonic anomaly as well as the anomalous upward flow over the western TP. Otherwise, it is worth noting that the anomalous snow cover developed over the western plateau in spring will, in turn, cool the air column and further strengthen the upper level anomalous low, which may help the spring WTPSC to develop quickly.

As in Fig. 8, the composite difference patterns in spring (MAM) snow cover, meridional wind vertical shear (V100–V400) and 400-hPa vertical motion (omega) between low and high WNPI years (defined when WNPI is beyond the ∓0.70.7 standardized deviation) are presented (Fig. 9). The circulation patterns show similarity to those in Fig. 8. Associated with those ENSO related negative precipitation anomalies in western north Pacific and Maritime Continent, anomalous upward motion and positive snow cover occupy the western TP. These results further point out the importance of this ENSO associated precipitation in western north Pacific and Maritime Continent.

To further verify the above speculation, the ECHAM (v5.4) model is applied. Given an observational SST, realistic climatological upper winds in the Eurasian continent and Pacific regions can be simulated by this model (Fig. 10a). Then the composite SSTA for El Niño and La Niña events in Pacific are added to the spring (MAM) mean SST field. By analyzing the difference of EXP-TPA (EN) and EXP-TPA (LN) runs, the simulated circulation pattern displays similarity to the observed one (Fig. 7a). In Pacific region, two anomalous anticyclones straddle along the tropical center and eastern Pacific while a cyclonic anomaly over Aleutian Islands (Fig. 10b). Over the TP regions, an evident cyclonic anomaly dominates there, as shown in Fig. 7a. Moreover, the SSTA forced model results of 400-hPa vertical motion and precipitation over TP are presented in Fig. 11a, b. Striking dipole modes are shown in these figures, with anomalous upward motion

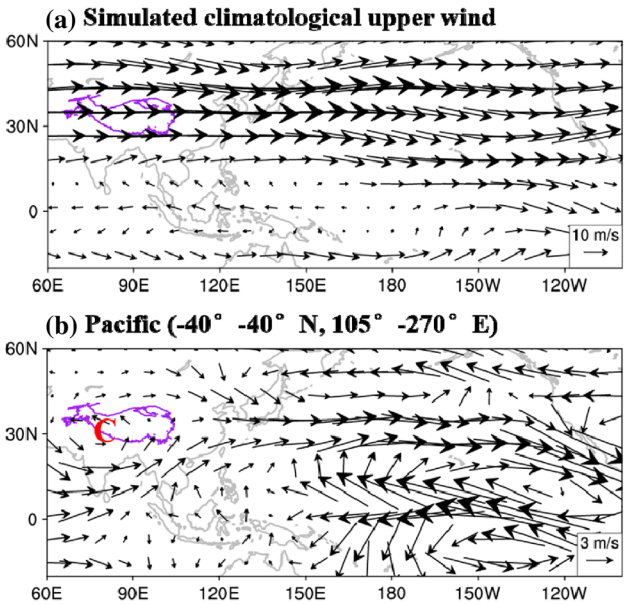

Fig. 10 The results simulated by ECHAM5. **a** The simulated climatological upper wind (200-hPa, UV) (m/s), **b** the upper wind (200-hPa, UV) anomalies (m/s) simulated by ENSO associated spring SST forcing in Pacific. The purple curve represents the area above 3000 m. The letter C denotes cyclonic circulation center

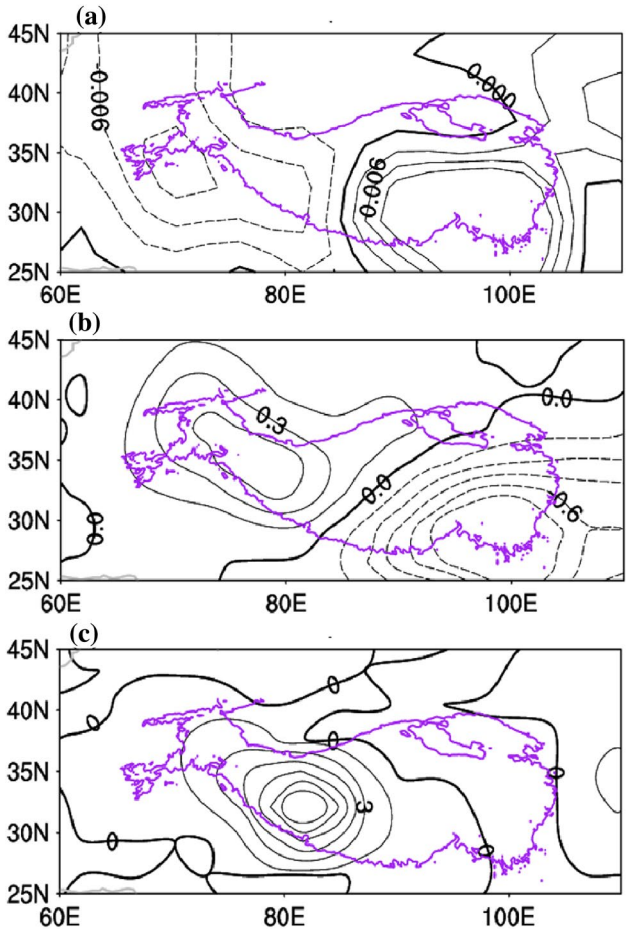

Fig. 11 As in Fig. 10, but for the model results of **a** the middle level vertical motion (400-hPa omega) (Pa/s), **b** the precipitation (kg/m^2 day), and **c** the snow depth (mm). The purple curve represents the area above 3000 m

and positive precipitation in western TP while weak downward motion and negative precipitation in eastern TP (Fig. 11a, b), which are consistent with the observations (Figs. 7c, 8c). Then the corresponding model result of snow depth is shown in Fig. 11c (Snow cover is not in the model outputs, so snow depth is used). Positive snow depth abnormity is presented over the central and western TP, with its position moving slight eastward. Considering the otherness between snow cover and snow depth, it is understandable that the model results of snow depth center shifts slightly.

The model results revealed above further suggest that the anomalous circulation patterns over TP and the WTPSC anomalies are the responses to tropical Pacific SST forcing. During this process, the ENSO associated SST and convection anomalies in the entire Pacific may contribute to the establishment of the WTPSC in spring.

4.2 Spring WTPSC influence on the Yellow River summer rainfall

The above analyses have proved that the spring WTPSC can be affected by ENSO. Then, how can such ENSO associated WTPSC abnormity in spring influence the following summer precipitation? The spring (MAM) and summer (JJAS) WTPSI (the mean snow cover in the area bounded by 33°N–43°N and 70°E–78°E) for the past 45 years are presented in Fig. 12. The in-phase relationship among them is detected (correlation = 0.58, exceeding the 99% confidence level), which indicates that the ENSO related spring WTPSC may continue to summer. Then, how can this WTPSC persist through summer and affect the Yellow River summer precipitation?

From Fig. 3c, the relationship between ENSO and the WTPSC becomes stronger in summer, which means that the ENSO associated SST and convection anomalies may also impact the TP circulation pattern in summer. Besides, the composite difference maps in TP snow cover and albedo between warm and cold ENSO events are shown (Fig. 13). For these variables, large areas of significant positive correlations occupy the western TP from the late spring [April–June (AMJ)] to summer (JJAS), in accordance with the WTPSC key region shown in Fig. 3. This suggests that once the anomalous spring WTPSC has been induced over western TP, the snow-albedo effect will be stimulated to maintain the WTPSC from spring to summer. The main process is proposed as follows: the anomalous cyclonic circulation over TP as well as the abnormal upward motion may favor the anomalous convective activities in western TP, which may contribute to the snow cover increase there. The more WTPSC tends to strengthen the albedo effect and decrease the net shortwave radiation near surface, which in turn, leads to a stronger WTPSC. It is this positive feedback process that further strengthens the WTPSC until summertime.

Above, we have proved that the ENSO associated WTPSC may endure from spring to summer. Then how can this WTPSC in summertime contribute to the Yellow River summer rainfall anomaly? To verify this question, the upper wind (200-hPa, UV) and geopotential height (200-hPa, Z)

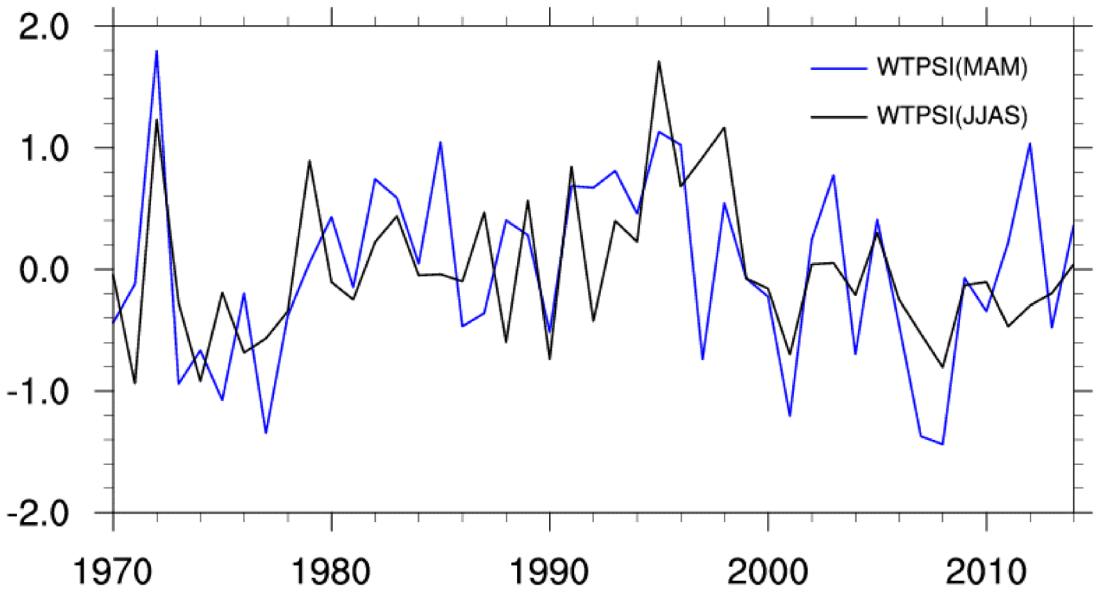

Fig. 12 Detrended time series of the normalized WTPSI for (blue) spring (MAM) and (black) summer (JJAS). The WTPSI definition can be found in Fig. 3

anomalies regressed against the WTPSC (JJAS) are revealed (Fig. 14a). A wave train pattern induced by the WTPSC anomaly is shown in upper troposphere propagating northeastward, with an anomalous low pressure center located over northeast China. This circulation structure is highly concordant with the conclusion of Wu et al. (2015). Besides, the lower wind (850-hPa, UV) is also regressed against the WTPSC (JJAS) in Fig. 14b. Another wave train is discovered to the south of TP along the low level southwesterly, similar to the model result by Wang et al. (2008). However, the low level wave train by Wang is derived from the entire warming TP, which may be somewhat different from our result. Influenced by these two wave trains, an anomalous low pressure center prevails in northeast China. This circulation pattern in northeast China is similar in both upper and lower level, forming a barotropic structure. To the southwest side of the anomalous low pressure in northeast China, the abnormal northerly wind may bring large volumes of dry cold air with little moisture to the Yellow River, leading to the anomalous drought there. Thus, the ENSO associated summer WTPSC may impact the Yellow River summer rainfall.

5 Conclusion and discussion

Climate anomalies (i.e., severe droughts, floods and heat wave activities) in the Yellow River region experience evident interannual variations (Zhai et al. 1999; Gong and Wang 2000; Ren et al. 2005; Wang and Ding 2006; Ding et al. 2007; Wu et al. 2012b), yet to what extent and how ENSO would contribute to such interannual variations remain an outstanding issue. Based on the climate effect of ENSO and the WTPSC, we analyze the influence of ENSO on the WTPSC and their combined effects on interannual

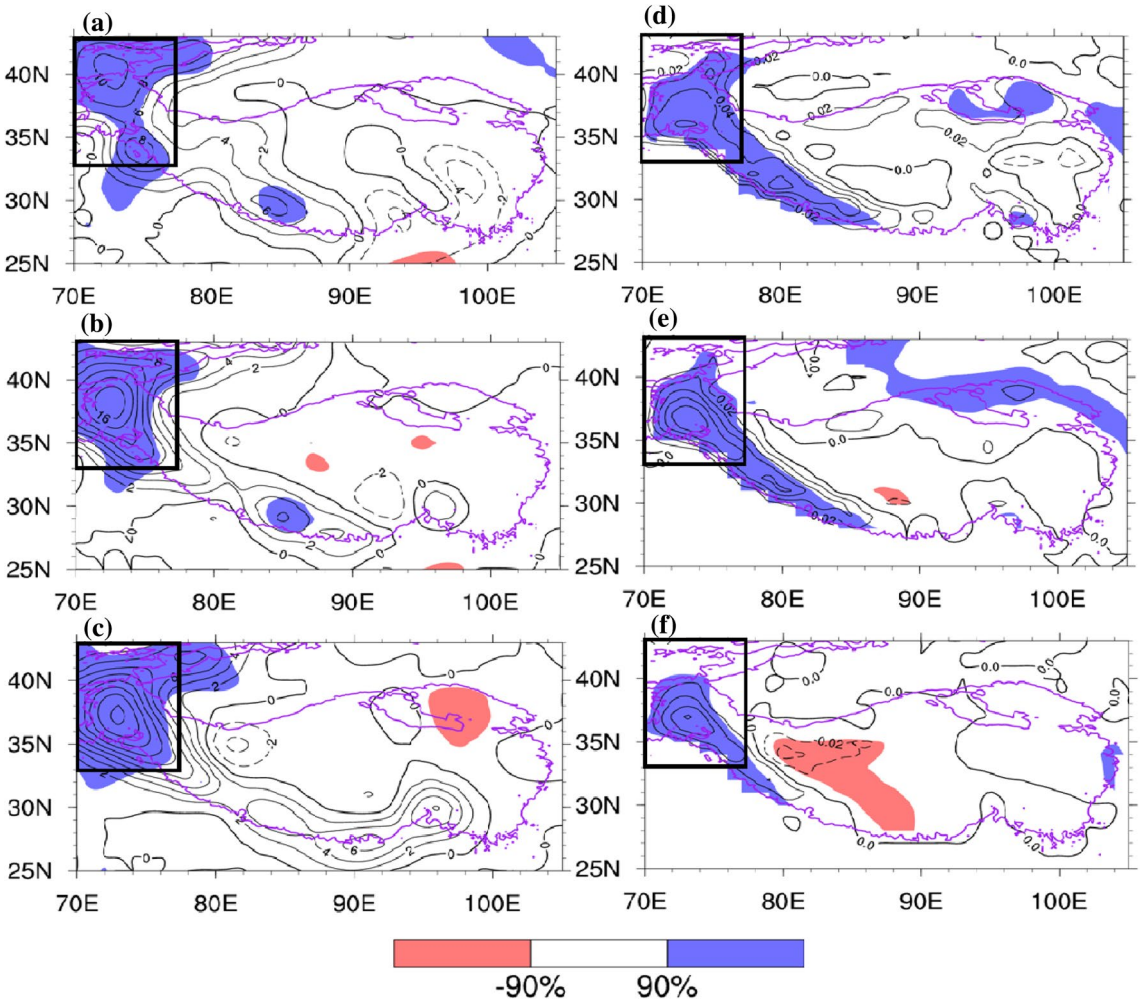

Fig. 13 Composite differences of the **a**–**c** snow cover (%), **d**–**f** albedo for **a, d** late spring [April-June (AMJ)], **b, e** early summer [May–July (MJJ)] and **c, f** summertime (JJAS) between the warm and cold ENSO events. The purple curve represents the area above 3000 m. The positive (negative) values significant at the 90% confident level are shaded with blue (red)

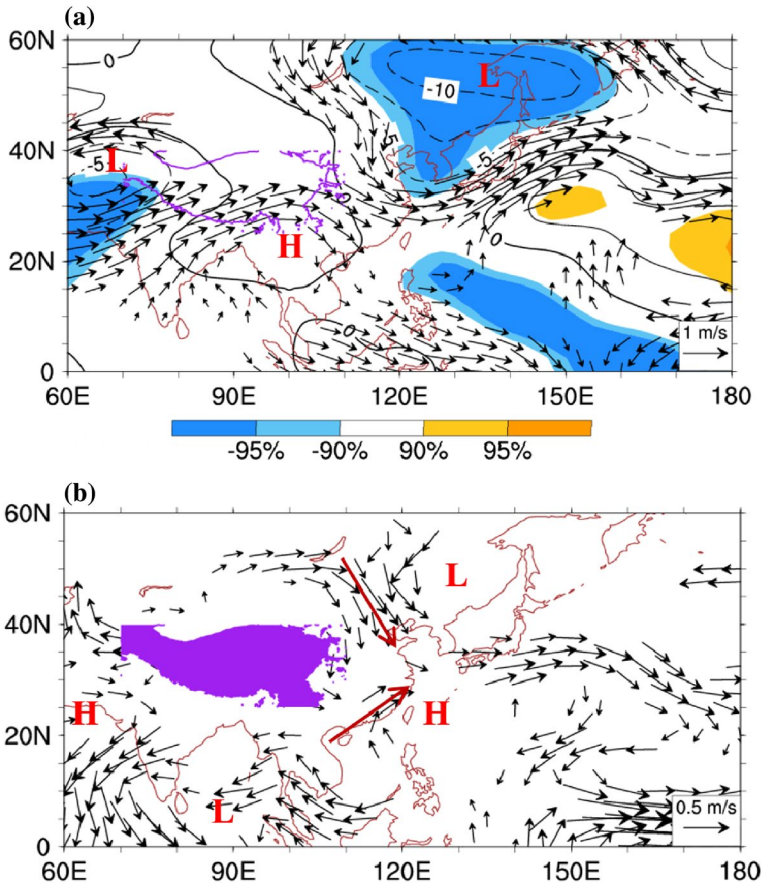

Fig. 14 **a** JJAS upper level geopotential height (m) and wind (m/s) (200 hPa) regressed against the detrended WTPSI. **b** As in **a** but for the lower level wind (m/s) (850 hPa). The purple curve and shading represent the area above 3000 m. The positive (negative) values significant at the 90% and 95% confident level are shaded with light and dark yellow (blue). The vectors represent statistically significant at 90% confidence level. The letter H and L denote high and low pressure, respectively

variations of the Yellow River summer precipitation, during ENSO developing phase. The results of this study show that, via changing the variation of the WTPSC, the indirect effect of a developing ENSO may be crucial to the Yellow River summer precipitation variations.

For the physical mechanism, the possible processes are summarized as follows: The ENSO related SSTA and precipitation anomaly throughout the Pacific region in its developing phase is quite crucial to the establishment of the WTPSC, which may contribute to the rainfall anomaly in the Yellow River region. The El Niño associated heating may arise anomalous deep convection in eastern Pacific and weaken the Walker Circulation (Feng and Li 2013; Feng et al. 2013; Guo and Li 2016), which may give rise to the anomalous downward motion as well as the suppressed precipitation abnormity in tropical western north Pacific and Maritime Continent. Such ENSO related pattern throughout the entire Pacific, especially the negative convection anomalies in western north Pacific and Maritime Continent may lead to the anomalous upper level cyclone and anomalous upward flow over the western TP through the effect of Gill-response. This process may further persist until summer. Besides, once the WTPSC in spring has been developed, the positive snow-albedo feedback process will be stimulated, which may help the WTPSC to further strengthen in the summertime (JJAS) and contribute to the Yellow River summer rainfall via the eastward propagating wave trains in both upper and lower levels.

It should be pointed out that, on the interannual time scales, ENSO is the dominant mode in the tropics and may influence the year-to-year variations of the WTPSC. Actually, some other influential factors over a longer time scales may also exert impact on the WTPSC, such as the Pacific Decadal Oscillation, the Atlantic Multidecadal Oscillation and the Arctic sea ice (Garcia and Kayano 2008; Zhu and Yang 2003; Krishnan and Sugi 2003; Dong and Dai 2015; Joshi and Rai 2015). As a result, except for the significant interannual variations, the WTPSC also shows multi-scale variations (Fig. 3b). Accompanied by such longtime scale variability, the WTPSI variation is out of step with the Niño 3.4 index (MAM) in a few years, in spite of an overall significant positive correlation. These exceptions may further influence the climate change in East Asian. Then, whether this interdecadal variation of the WTPSC may affect the ENSO-WTPSC relationship and what are the forcing factors still need further study, which may be quite crucial and indispensable in advancing the ability of weather forecast and disaster prevention in China.

Acknowledgements We thank the Global Snow Lab (Rutgers University) for providing the snow cover area extent data. This work is jointly supported by the National Key Research & Development Program of China (Grant No. 2016YFA0601801), the National Natural Science Foundation of China (NSFC) (Grant No. 91637312), the Ministry of Science and Technology of China (Grant Nos. 2015CB453201 and 2015CB953904) and the NSFC (Grant Nos. 91437216 and 41575075).

References

Chang CP, Zhang YS, Li T (2000) Interannual and interdecadal variations of the East Asian summer monsoon and tropical Pacific SSTs. Part I: roles of the subtropical ridge. J Clim 13(24):4310–4325

Chen MY, Xie PP, Janowiak JE, Arkin PA (2002) Global Land Precipitation: A 50-yr monthly analysis based on gauge observations. J Hydrometeorol 3(3):249–266

Ding QH, Wang B (2005) Circumglobal teleconnection in the northern hemisphere summer*.J Clim 18(17):3483–3505

Ding YH, Ren GY, Zhao ZC, Xu Y, Luo Y, Li QP, Zhang J (2007) Detection, causes and projection of climate change over China: An overview of recent progress. Adv Atmos Sci 24(6):954–971

Dong B, Dai AG (2015) The influence of the interdecadal Pacific Oscillation on temperature and precipitation over the globe. Clim Dyn 45:2667–2681

Dong BW, Valdes PJ (1998) Modelling the Asian summer monsoon rainfall and Eurasian winter/spring snow mass. Q J R Meteorol Soc 124(552):2567–2596

Duan AM, Wu GX (2005) Role of the Tibetan Plateau thermal forcing in the summer climate patterns over subtropical Asia. Clim Dyn 24:793–807

Feng S, Hu Q (2004) Variations in the teleconnection of ENSO and summer rainfall in northern China: a role of the indian summer monsoon. J Clim 17(24):4871–4881

Feng J, Li JP (2013) Contrasting impacts of two types of ENSO on the boreal spring Hadley circulation. J Clim 26:4773–4789

Feng J, Chen W, Tam CY, Zhou W (2011) Different impacts of El Niño and El Niño Modoki on China rainfall in the decaying phases. Int J Climatol 31(14):2091–2101

Feng J, Li JP, Xie F (2013) Long-term variation of the principal mode of boreal spring Hadley Circulation linked to SST over the Indo-Pacific Warm Pool. J Clim 26:532–544

Feng J, Li JP, Zheng F, Xie F, Sun C (2016) Contrasting impacts of developing phases of two types of El Niño on Southern China rainfall. J Meteorol Soc Jpn 94(4):359–370

Garcia SR, Kayano MT (2008) Climatological aspects of Hadley, Walker and monsoon circulations in two phases of the Pacific Decadal Oscillation. Theor Appl Climatol 91:117–127

Gill AE (1980) Some simple solutions for heat-induced tropical circulation. Q J R Meteorol Soc 106(449):447–462

Gong DY, Wang SW (2000) Severe summer rainfall in China associated with enhanced global warming. Clim Res 16(1):51–59

Guo YP, Li JP (2016) Impact of ENSO events on the interannual variability of Hadley circulation extents in boreal winter. Adv Clim Change Res 7(1):46–53

Guo QY, Wang JQ (1988) A comparative study on summer monsoon in China and India. J Trop Meteorol 4:53–60 **(in Chinese)**

Huang G (2004) An index measuring the interannual variation of the East Asian summer monsoon—the EAP index. Adv Atmos Sci 21:41–52

Huang RH, Wu YF (1989) The influence of ENSO on the summer climate change in China and its mechanisms. Adv Atmos Sci 6:21–32

Huang G, Liu Y, Huang RH (2011) The interannual variability of summer rainfall in the arid and semiarid regions of northern china and its association with the northern hemisphere circumglobal teleconnection. Adv Atmos Sci 28(2):257–268

Joshi MK, Rai A (2015) Combined interplay of the Atlantic multidecadal oscillation and the interdecadal Pacific oscillation on rainfall and its extremes over Indian subcontinent. Clim Dyn 44(11–12):3339–3359

Ju JH, Slingo J (1995) The Asian summer monsoon and ENSO. Q J R Meteorol Soc 121(525):1133–1168

Kalnay E, Kanamitsu M, Kistler R, Collins W, Deaven D, Gandin L, Iredell M, Saha S, White G, Woollen J, Zhu Y, Chelliah M, Ebisuzaki W, Higgins W, Janowiak J, Mo KC, Ropelewski C, Wang J, Leetmaa A, Reynolds R, Jenne R, Joseph D (1996) The NCEP/NCAR 40-year reanalysis project. Bull Amer Meteorol Soc 77(3):437–472

Kawamura R (1998) A possible mechanism of the Asian summer monsoon-ENSO coupling. J Meteorol Soc Jpn 76:1009–1027

Kripalani RH, Kulkarni A (1997) Rainfall variability over southeast Asia—connections with Indian monsoon and ENSO extremes: New perspective. Int J Climatol 17:1155–1168

Kripalani RH, Singh SV (1993) Large-scale aspects of India-China summer monsoon rainfall. Adv Atmos Sci 10:72–84

Krishnan R, Sugi M (2003) Pacific decadal oscillation and variability of the Indian summer monsoon rainfall. Clim Dyn 21:233–242

Li JP (2009) Tropical pacific and its global impacts. Theor Appl Climatol 97(1–2):1–2

Li JP, Sun C, Jin FF (2013) NAO implicated as a predictor of northern hemisphere mean temperature multidecadal variability. Geophys Res Lett 40(20):5497–5502

Liang XZ, Wang WC (1998) Association between China monsoon rainfall and tropospheric jets. Q J R Meteorol Soc Lond 124:2597–2623

Lin H, Wu ZW (2011) Contribution of the autumn Tibetan Plateau snow cover to seasonal prediction of North American winter temperature. J Clim 24:2801–2813

Liu YM, Wu GX (2004) Progress in the study on the formation of the summertime subtropical anticyclone. Adv Atmos Sci 21:322–342

Liu YM, Wu GX, Ren RC (2004) Relationship between the subtropical anticyclone and diabatic heting. J Clim 17:682–698

Liu YM, Bao Q, Duan AM, Qian ZA, Wu GX (2007) Recent progress in the impact of the Tibetan Plateau on climate in China. Adv Atmos Sci 24(6):1060–1076

Liu G, Wu RG, Zhang YS, Nan SL (2014) The summer snow cover anomaly over the Tibetan Plateau and its association with simultaneous precipitation over the mei-yu-baiu region. Adv Atmos Sci 31(4):755–764

Liu G, Zhao P, Chen JM, Yang S (2015) Preceding factors of summer Asian-Pacific oscillation and the physical mechanism for their potential influences. J Clim 28(7):2531–2543

Matsuno T (1966) Quasi-geostrophic motions in the Equatorial area. J Meteorol Soc Jpn 44(1):25–42

Miyakoda K, Kinter JL, Yang S (2003) The role of ENSO in the South Asian monsoon and pre-monsoon signals over the Tibetan Plateau. J Meteorol Soc Jpn 81(5):1015–1039

Murakami T, Ding YH (1982) Wind and temperature changes over Eurasia during the early summer of 1979. J Meteorol Soc Jpn 60:183–196

Nitta T (1987) Convective activities in the tropical western Pacific and their impact on the northern hemisphere summer circulation. J Meteorol Soc Jpn 65:373–390

Poli P, Hersbach H, Dee DP, Berrisford P, Simmons AJ, Vitart F, Laloyaux P, Tan DGH, Peubey C, Thépaut JN, Trémolet

Y, Hólm EV, Bonavita M, Isaksen L, Fisher M (2016) ERA-20C: an atmospheric reanalysis of the 20th century. J Clim. doi:10.1175/JCLI-D-15-0556.1

Pu ZX, Xu L, Salomonson VV (2007) MODIS/Terra observed seasonal variations of snow cover over the Tibetan Plateau. Geophys Res Lett 34(6):137–161

Qian YF, Zheng YQ, Zhang Y, Miao MQ (2003) Responses of china's summer monsoon climate to snow anomaly over the Tibetan Tlateau. Int J Climatol 23(6):593–613

Ren GY, Guo J, Xu MZ, Chu ZY, Zhang L, Zou XK (2005) Climate changes of mainland China over the past half century. Acta Meteorol Sin 63(6):942–956

Ren XJ, Yang XQ, Chu CJ (2010) Seasonal variations of the synoptic-scale transient eddy activity and polar front jet over East Asia. J Clim 23(12):3222–3233

Robinson DA, Frei A (2000) Seasonal variability of northern hemisphere snow extent using visible satellite data. Prof Geogr 51:307–314

Robinson DA, Dewey KF, Heim RRJ (1993) Global snow cover monitoring: an update. Bull Am Meteorol Soc 74:1689–1696

Roeckner E, Bäuml G, Bonaventura L, Brokopf R, Esch M, Giorgetta M, Hagemann S, Kirchner I, Kornblueh L, Manzini E, Rhodin A, Schlese U, Schulzweida U, Tompkins A (2003) The atmospheric general circulation model ECHAM5. Part I: Model description. Max Planck Institute for Meteorology Rep. 349, 127 pp. Available from MPI for Meteorology, Bundesstr. 53, 20146 Hamburg, Germany

Ropelewski CF, Halpert MS (1987) Global and regional scale precipitation patterns associated with the El Niño/Southern Oscillation. Mon Weather Rev 115(8):1606–1626

Shaman J, Tziperman E (2005) The effect of ENSO on Tibetan Plateau snow depth: a stationary wave teleconnection mechanism and implications for the South Asian monsoons. J Clim 18(12):2067–2079

Shukla J, Paolino DA (1983) The Southern Oscillation and long-range forecasting of the summer monsoon rainfall over India. Mon Weather Rev 111(9):1830–1837

Smith TM, Reynolds RW, Peterson TC, Lawrimore J (2008) Improvements to NOAA's historical merged land–ocean surface temperature analysis (1880–2006). J Clim 21:2283–2295. doi:10.1175/2007JCLI2100.1

Wang B, Ding QH (2006) Changes in global monsoon precipitation over the past 56 years. Geophys Res Lett 33(6):272–288

Wang B, Wu RG, Fu XH (2000) Pacific–East Asian teleconnection: how does ENSO affect East Asian climate?* J Clim 13(9):1517–1536

Wang B, Wu RG, Lau KM (2001) Interannual variability of the Asian summer monsoon: contrasts between the Indian and the western North Pacific-East Asian monsoons. J Clim 14:4073–4090

Wang B, Wu RG, Li T (2003) Atmosphere–warm ocean interaction and its impacts on Asian–Australian monsoon variation. J Clim 16:1195–1211

Wang B, Bao Q, Hoskins B, Wu GX, Liu YM (2008) Tibetan Plateau warming and precipitation changes in East Asia. Geophys Res Lett 35(14):63–72

Webster PJ, Yang S (1992) Monsoon and ENSO: selectively interactive systems. Q J R Meteorol Soc 118(507):877–926

Wu G, Liu Y (2003) Summertime quadruplet heating pattern in the subtropics and the associated atmospheric circulation. Geophys Res Lett 30(5):1201. doi:10.1029/2002GL016209

Wu RG, Wang B (2002) A contrast of the East Asian summer monsoon-ENSO relationship between 1962–77 and 1978–93. J Clim 15:3266–3279

Wu GX, Zhang YS (1998) Tibetan Plateau forcing and the timing of the monsoon onset over South Asia and the South China Sea. Mon Weather Rev 126:913–927

Wu GX, Li W, Guo H, Liu H, Xue J, Wang Z (1997) Sensible heat driven air-pump over the Tibetan Plateau and its impacts on the Asian summer monsoon. Collections on the memory of Zhao Jiuzhang. Chinese Science Press, Beijing

Wu GX, Liu YM, Wang TM, Wan RJ, Liu X, Li WP, Wang ZZ, Zhang Q, Duan AM, Liang XY (2007) The influence of mechanical and thermal forcing by the Tibetan Plateau on Asian climate. J Hydrometeorol 8(4):770–789

Wu ZW, Wang B, Li JP, Jin FF (2009) An Empirical seasonal prediction model of the East Asian summer monsoon using ENSO and NAO. J Geophys Res 114:D18120. doi:10.1029/2009JD011733

Wu ZW, Li JP, Jiang ZH, Ma TT (2012a) Modulation of the Tibetan Plateau snow cover on the ENSO teleconnections: from the East Asian summer monsoon perspective. J Clim 25(25):2481–2488

Wu ZW, Jiang ZH, Li JP, Zhong SS, Wang LJ (2012b) Possible association of the western Tibetan Plateau snow cover with the decadal to interdecadal variations of northern China heatwave frequency. Clim Dyn 39(9–10):2393–2402

Wu ZW, Zhang P, Chen H, Li Y (2015) Can the Tibetan Plateau snow cover influence the interannual variations of Eurasian heat wave frequency? Clim Dyn 46(11–12):3405–3417

Xie SP, Hu KM, Hafner J, Tokinaga H, Du Y, Huang G, Sampe T (2009) Indian Ocean Capacitor Effect on Indo-Western Pacific Climate during the Summer following El Niño. J Clim 22(3):730–747

Yang S (1996) ENSO-snow-monsoon associations and seasonal-interannual predictions. Int J Climatol 16(2):125–134

Yang FL, Lau KM (2004) Trend and variability of China precipitation in spring and summer: linkage to sea-surface temperatures. Int J Climatol 24:1625–1644

Yatagai A, Yasunari T (1995) Interannual variations of summer precipitation in the arid/semi-arid regions in China and Mongolia: their regionality and relationship to the Asian monsoon. J Meteorol Soc Jpn 73:909–923

Zhai PM, Sun AJ, Ren FM, Liu XN, Gao B, Zhang Q (1999) Changes of climate extremes in China. Clim Change 42(1):203–218

Zhang RH (1999) The role of Indian summer monsoon water vapor transportation on the summer rainfall anomalies in the northern part of China during the El Niño mature phase. Plateau Meteorol 18:567–574 **(in Chinese)**

Zhang SL, Tao SY (2001) Influences of snow cover over the Tibetan Plateau on Asian summer monsoon. Chin J Atmos Sci 25:372–390 **(in Chinese)**

Zhang RH, Sumi A, Kimoto M (1999) A diagnostic study of the impact of El Nino on the precipitation in China. Adv Atmos Sci 16:229–241

Zhang YS, Li T, Wang B (2004) Decadal change of the spring snow depth over the Tibetan Plateau: the associated circulation and influence on the East Asian summer monsoon. J Clim 17(14):2780–2793

Zheng F, Li JP, Li YJ, Zhao S, Deng DF (2016) Influence of the summer NAO on the spring-NAO-based predictability of the East Asian summer monsoon. J Appl Meteorol Climatol 55(7):1459–1476

Zhu YM, Yang XQ (2003) Relationships between Pacific Decadal Oscillation and climate variabilities in China. J Meteorol Soc Jpn 61(6):641–654